Theor Chem Acc (2001) 106:178–187
DOI 10.1007/s002140100263

Theoretical
Chemistry Accounts

Regular article

Molecular integrals by numerical quadrature. I. Radial integration

Roland Lindh[1], **Per-Åke Malmqvist**[2], **Laura Gagliardi**[3]

[1] Department of Chemical Physics, Chemical Center, P.O. Box 124, 221 00 Lund, Sweden
[2] Department of Theoretical Chemistry, Chemical Center, P.O. Box 124, 221 00 Lund, Sweden
[3] Dipartimento di Chimica Fisica ed Inorganica, Università di Bologna, Viale Risorgimento 4, 40136 Bologna, Italy

Received: 30 August 2000 / Accepted: 21 December 2000 / Published online: 3 April 2001

Abstract. This article presents a numerical quadrature intended primarily for evaluating integrals in quantum chemistry programs based on molecular orbital theory, in particular density functional methods. Typically, many integrals must be computed. They are divided up into different classes, on the basis of the required accuracy and spatial extent. Ideally, each batch should be integrated using the minimal set of integration points that at the same time guarantees the required precision. Currently used quadrature schemes are far from optimal in this sense, and we are now developing new algorithms. They are designed to be flexible, such that given the range of functions to be integrated, and the required precision, the integration is performed as economically as possible with error bounds within specification. A standard approach is to partition space into a set of regions, where each region is integrated using a spherically polar grid. This article presents a radial quadrature which allows error control, uniform error distribution and uniform error reduction with increased number of radial grid points. A relative error less than 10^{-14} for all s-type Gaussian integrands with an exponent range of 14 orders of magnitude is achieved with about 200 grid points. Higher angular l quantum numbers, lower precision or narrower exponent ranges require fewer points. The quadrature also allows controlled pruning of the angular grid in the vicinity of the nuclei.

Key words: Numerical quadrature – Molecular orbital theory – Density functional theory

1 Introduction

Quantum chemistry of polyatomic systems has usually relied on fast evaluation of analytic formulae, made possible by the use of Gaussian basis sets introduced by Boys [1] and developed into highly efficient algorithms such as the McMurchie–Davidson method [2], the Obara–Saika method [3] and the Rys–Gauss quadrature [4–6]. However, the increasingly important density functional theory (DFT) requires systematic evaluation of integrals of a complicated nature, for which there are no basis functions that allow simple closed formulae, but whose integrands are easily evaluated at arbitrary points in space. Such integrals are then best computed by numerical quadrature. In 1988, Becke [7] proposed the partitioning of the molecular integral into single-center components, each of which was evaluated by numerical quadrature using spherical polar coordinates. This is not necessarily the best strategy, but it is a simple and well-defined approach which has been adopted by most DFT programs. However, the radial integration formula used by Becke gives only a five- to six-figure accuracy of the integrals. Better schemes have been introduced. Some important contributions are those of Murray, Handy and Laming [8], Treutler and Alrichs [9] and Mura and Knowles [10]. Also the angular integration has been much improved by the Lobatto (see, for example, Ref. [9]) and Lebedev approaches [11]. The partitioning technique has been studied [12], considerations of linear-scaling have attracted attention [13] and adaptive integration schemes have been suggested [12, 14, 15]. Nevertheless, it seems that the errors introduced by the radial integration are still unacceptably large in many applications and are not easily controlled by the user. Examples of shortcomings of the numerical quadrature are given by Tozer and Handy [16], in computing excitation energies to Rydberg states with a DFT approach, and by Mura and Knowles [10], who, in analyzing the error of the so-called LOG3 scheme, noted that the LiH and LiF molecules had to be eliminated from the test set owing to the poor precision of the integrals for these two molecules.

The present article suggests a rather simple and straightforward radial quadrature scheme to eliminate such problems. Each batch of integrands is characterized by the highest and lowest exponent of a set of Gaussian

Correspondence to: R. Lindh

functions, and the user, or rather the integration package, specifies that all integrals of a certain standard type should be integrated to within a certain accuracy. By explicit and simple formulae, integration points and weights are determined such that the numerical quadrature meets these requirements. The actual integrals to compute are, of course, not exactly of the standard type that defines the quality requirements (if they were, numerical quadrature would not be the preferred method). The assumption is just that the user will express his requirements in this form, which is also natural for such molecular orbital programs that are based on expansion in Gaussian basis sets.

The most common previous methods are reviewed in Sect. 2 and their errors are compared to analytic results. The design of the new quadrature is described in Sect. 3 and its performance is compared to that of previously used methods in Sect. 4. Finally, the article ends with a conclusion.

2 Review of some standard radial quadratures

The accuracy of numerical integration schemes for DFT is usually assessed by the error in the integrated density and sometimes also the Slater–Dirac exchange functional for some set of molecules. In the former case, accurate results are obtained from analytic integrals; in the latter case the number of grid points in the numerical quadrature is increased until the evaluated integral appears to have reached a stable value. We have noted examples where an apparently stable value is in fact of quite poor accuracy.

Here, we follow a different approach, by simply studying the error of a test set of Gaussian integrands rather than molecular integrals for some set of molecules. The reason is that we wish the integrals to be reliable for any basis set, including possibly very sharp core orbitals or extremely diffuse ones, or Rydberg funtions. This means that the grid must be basis-set dependent, and we wish to find simple criteria for obtaining close-to-optimal integration formulae, as defined by the precision requirements. We compute the integration error in the self-overlap integral of normalized Gaussians as a function of the Gaussian exponent.

The exponents used in the 6-31G and the ANO-L basis sets for the first 30 elements are shown in Fig. 1. The logarithm of the Gaussian exponent is seen to lie in the range -3 to 7. The lower exponents are especially important for alkali and rare-earth metals. The lower range of -3 is expected to be unchanged if other elements of the periodic table are included and it will have to be lowered only for extreme cases such as Li^- or for the higher Rydberg states. The high end of the range must be increased for heavier elements, where the logarithm of the exponent may become as large as 12–14, or even higher in relativistic work if a point nucleus is assumed.

In the following, the integration error of various methods will be studied for the exponent range 10^{-5}–10^{10}.

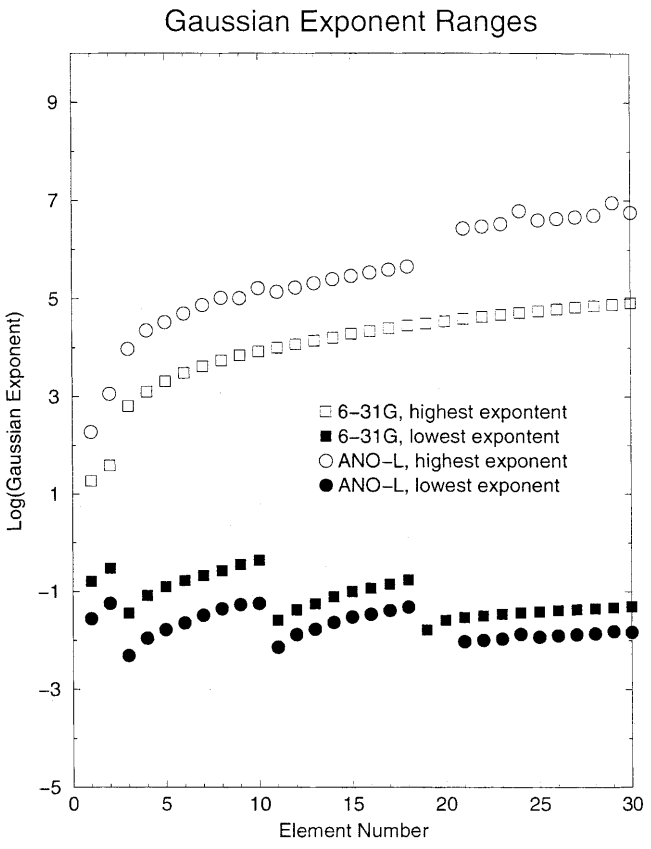

Fig. 1. The logarithm of the highest and lowest Gaussian exponents of the 6-31G and ANO-L basis sets for the first 30 elements of the periodic table

2.1 The Becke scheme

The scheme of Becke [7] is based on the coordinate transformation

$$r = \alpha \frac{1+x}{1-x} \tag{1}$$

using points in $-1 \leq x \leq 1$ and standard Gauss–Chebyshev quadrature of the second kind for the x-space quadrature. α is a parameter corresponding to the midpoint of the integration interval at $x = 0$, which was chosen to be half the Bragg–Slater radius, except for hydrogen, for which the whole Bragg–Slater radius was used.

2.2 The Murray, Handy and Laming scheme

The EM grid of Murray et al. [8] is defined from the Euler–Maclaurin approach by the transformation

$$r = \alpha \left(\frac{x}{1-x}\right)^m \quad . \tag{2}$$

Use of the Euler–Maclarin formula converts the integral to a sum over an equidistant grid, plus correction terms that depend on the derivatives at the end of the interval. Depending on the value m, a few of these derivatives are

automatically zero. The rest are ignored, yielding a formula with equal weights and yet of high order. However, for any given number of points, it cannot be generally assumed that increasing orders give higher accuracy. Ultimately, the break-even step size gets smaller and smaller when m is increased, and the Euler–Maclaurin series does not converge.

Murray et al. chose the exponent $m = 2$, and the α is the Bragg–Slater radius.

2.3 The Treutler and Alrichs scheme

The so-called M4T2 scheme of Treutler and Alrichs [9] is based on the transformation

$$r = \frac{\alpha}{\ln 2}(1+x)^{0.6}\ln\left(\frac{2}{1-x}\right) \ , \tag{3}$$

using standard Gauss–Chebyshev quadrature of the second kind for the integration over x. The scaling depends on the atom type and is in the range 0.8–2.0.

2.4 The Mura and Knowles scheme

The so-called LOG scheme of Mura and Knowles [10] is based on the transformation

$$r = -\alpha\ln(1-x^m) \ , \tag{4}$$

with $0 \le x \le 1$ and a simple Gauss quadrature over x. Recommended values are $m = 3$ and $\alpha = 5.0$ (7.0 for alkali and rare-earth metals).

2.5 Properties of existing radial quadratures

The precision of the four methods (Becke, EM, M4T2 and LOG3) was studied by evaluating the integral

$$\frac{2\alpha^{(l+3)/2}}{\Gamma[(l+3)/2]}\int_0^\infty r^l \exp(-\alpha r^2) r^2 \, \mathrm{d}r = 1 \ . \tag{5}$$

Such integrals arise, for example as the overlap of Gaussian basis functions with l equal to the sum of the two angular quantum numbers and α equal to the sum of the exponents. In all cases, we used an exponent range $\alpha \in [10^{-5}, 10^{10}]$.

First, integrals with $l = 0$, corresponding to s-type Gaussians, were evaluated using radial grids with 50, 100 and 200 points. Secondly, a grid with 100 points was used with $l = 0, 2, 4, 20$ and 40. The lower l values will of course occur simply as basis function products. The very high l values may occur in some schemes, where the space is subdivided into very nonspherical regions.

The results of the test are presented graphically in Figs. 2 and 3, where the logarithm of the computed integrated error is plotted as a function of the logarithm of the Gaussian exponent.

In the first test (with $l = 0$), the M4T2 and the LOG3 schemes give almost the same precision, down to errors of about 10^{-12}. The better accuracy of the LOG3 scheme in the middle exponent range, where the errors are already very small, is probably not important. The EM and Becke schemes are similar, but the former is much better for low exponents. All the radial quadratures have a short high-accuracy range (logarithm of relative error smaller than 10^{-10}) for grids of 50 points. The M4T2 and LOG3 scheme have here a wider range of accuracy compared to the EM and Becke schemes (3 orders of magnitude difference of the Gaussian exponent compared to about 1 order). As the number of grid points is increased, we note again that the EM and Becke schemes, although not completely identical, are similar. While the EM and Becke schemes show a more or less uniform accuracy improvement over the whole Gaussian exponent range, the M4T2 and LOG3 schemes place virtually all the improvement in the range of contracted Gaussian functions. The rate of improvement in the diffuse range for the M4T2 and LOG3 schemes seems to be so slow that an apparently stable result, with respect to grid size, could easily be mistaken to indicate an accurate result. The larger set of 200 quadrature points gives a range of accuracy better than 10^{-10} of about 4–5 orders of magnitude difference of the Gaussian exponent regardless of the scheme.

In the second test, the error for the EM and Becke schemes improves with higher angular momentum (up to $l = 4$ approximately), but it does not improve for M4T2 and LOG3. On the other hand, the latter methods have more or less the same precision regardless of the angular momentum. This is a bit surprising – an increase in the angular momentum means that the functions fade faster close to the nuclei and could be integrated accurately with fewer grid points. For the same reason, we would expect to see an extension in the accuracy range as we increase the angular momentum. This is indeed observed for the Becke and EM schemes. The reason for this not being observed for the M4T2 and LOG3 schemes is that these schemes have crowded the quadrature points such that the computed accuracy is already of machine accuracy, or better, in the high-accuracy range. Thus, as the angular momentum is increased, no improvement can be observed, since the numerical experiment is limited by the machine accuracy. As for the very high angular momentum functions, all quadratures investigated here exhibit a small and narrow range in which accuracy is achieved.

As will be seen shortly, the performance of the radial integration scheme can be much improved. That there is also a need for such improvement in existing DFT programs is shown already by two cases mentioned earlier, and we may add the fact that computation of the nuclear gradient can be sensitive to the orientation of the atomic grids. The list of cases could, of course, be extended at will by studies of heavy elements, NMR studies, anionic systems or Rydberg states; however, the

►

Fig. 2. The logarithm of the integrated error as a function of the logarithm of the Gaussian exponent as obtained for 50, 100 and 200 radial quadrature points for **a** the Becke scheme, **b** the EM scheme, **c** the M2T4 scheme and **d** for the LOG3 scheme

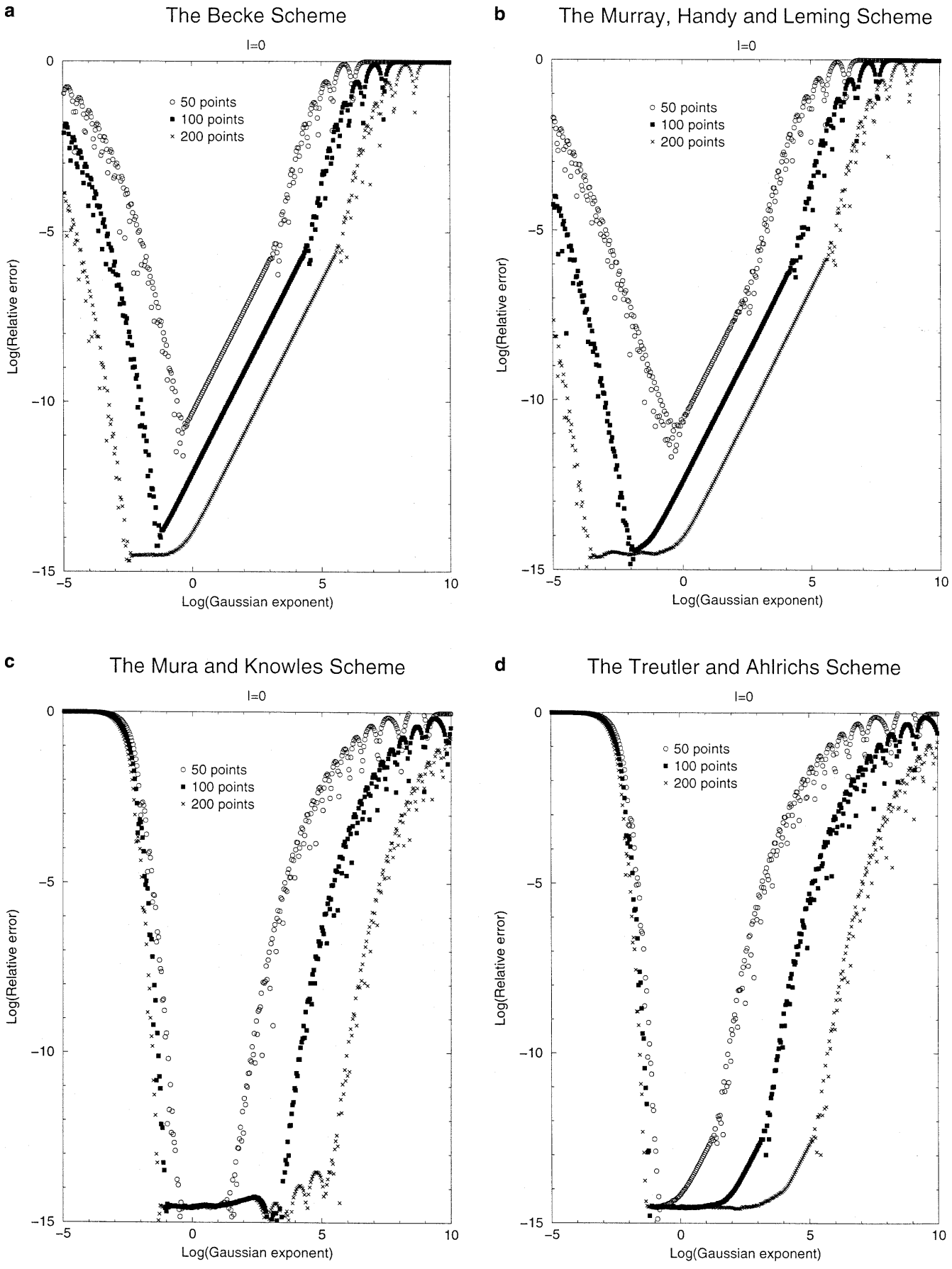
a
The Becke Scheme
l=0
50 points
100 points
200 points
Log(Relative error)
Log(Gaussian exponent)
b
The Murray, Handy and Leming Scheme
l=0
50 points
100 points
200 points
Log(Relative error)
Log(Gaussian exponent)
c
The Mura and Knowles Scheme
l=0
50 points
100 points
200 points
Log(Relative error)
Log(Gaussian exponent)
d
The Treutler and Ahlrichs Scheme
l=0
50 points
100 points
200 points
Log(Relative error)
Log(Gaussian exponent)

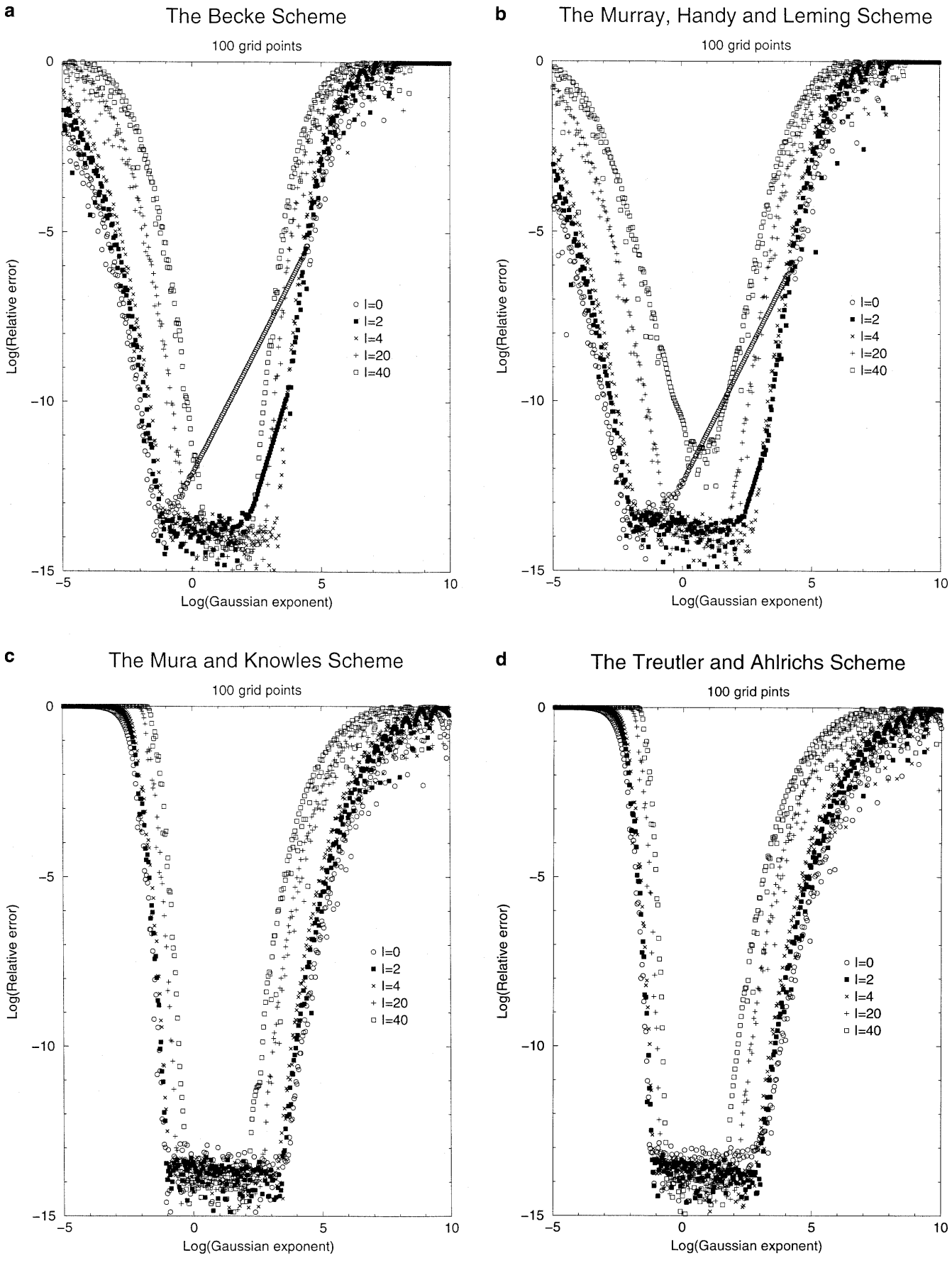
a
The Becke Scheme
100 grid points
Log(Relative error)
Log(Gaussian exponent)
l=0
l=2
l=4
l=20
l=40
b
The Murray, Handy and Leming Scheme
100 grid points
Log(Relative error)
Log(Gaussian exponent)
l=0
l=2
l=4
l=20
l=40
c
The Mura and Knowles Scheme
100 grid points
Log(Relative error)
Log(Gaussian exponent)
l=0
l=2
l=4
l=20
l=40
d
The Treutler and Ahlrichs Scheme
100 grid pints
Log(Relative error)
Log(Gaussian exponent)
l=0
l=2
l=4
l=20
l=40

◀

Fig. 3. The logarithm of the integrated error as a function of the logarithm of the Gaussian exponent of $l = 0$ (product of s functions), $l = 2$ (product of p functions), $l = 4$ (product of d functions), $l = 20$ and $l = 40$ as obtained in a 100 radial quadrature points approach for **a** the Becke scheme, **b** the EM scheme, **c** the M2T4 scheme and **d** the LOG3 scheme

point has already been made, and it is obvious that for any fixed recipe there will be extreme cases that are handled poorly. It is also obvious that any of the four schemes studied so far could quite easily be modified to encompass any of the cases that were handled less well.

It is thus clear that one scheme cannot be regarded as more precise than another, unless perhaps if one scheme has a smaller integration error than the other in a very wide range of exponents in a study such as the one described earlier. In fact, our proposed scheme seems close to optimal in that sense, but our strongest argument for a new quadrature is the fact that it can be designed by reliable formulae to meet any specific demand on precision within any required exponent range and is thus easily adapted to the specific needs of any particular integrand, or group of integrands – up to the limits dictated by machine precision, of course.

However, the accuracy and the complexity of a DFT calculation depends only to a limited extent on the radial integration itself. An unsuitable partitioning scheme can make extreme demands on the precision of the angular integration and can yield radial integrands with sharp features that in themselves require a dense grid. In the literature it has been reported that numerical stability may require accurate integration of functions with up to $l = 60$. The size of a reasonable highest-l value depends on the sharpness of so-called switching functions. It is clear from the results exhibited here that the earlier studies of the partioning scheme must have disfavored the use of softer switching functions, owing to the lack of accuracy of the radial grid for these kinds of integrands. It may be that a more accurate radial grid will allow softer switching functions, which, in turn, will require lower l values for an accurate overall integration. Hence, the more accurate radial integration could effectively allow a smaller overall grid.

3 Theory: design of the new radial quadrature

3.1 Design criteria and the test set

The main thought is to have a point/weight generating formula that for any case within a broad range of possible applications could provide a quadrature scheme with specified properties. The minimum requirements are formulated in terms of a test set

$$T(m, \alpha_{\mathrm{L}}, \alpha_{\mathrm{H}}) \ , \tag{6}$$

consisting of the functions

$$f(r; m, \alpha) = r^{m+2} \mathrm{e}^{-\alpha r^2} \ , \tag{7}$$

where m is a small integer larger than -3 and α is in the range $\alpha_{\mathrm{L}} \leq \alpha \leq \alpha_{\mathrm{H}}$ for $f \in T(m, \alpha_{\mathrm{L}}, \alpha_{\mathrm{H}})$. This set then represents the possible integrands.

The integral

$$I^{(m)}(\alpha) = \int_0^\infty r^{m+2} \mathrm{e}^{-\alpha r^2} \, \mathrm{d}r \tag{8}$$

is positive. We wish to find $\{r_k, w_k\}$ such that the quadrature

$$S^{(m)}(\alpha) = \sum_k w_k f(r_k; m, \alpha) \tag{9}$$

has a relative error, $R^{(m)}$, within specified limits for all functions in the test set:

$$1 - R^{(m)} \leq \frac{S^{(m)}(\alpha)}{I^{(m)}(\alpha)} \leq 1 + R^{(m)} \ . \tag{10}$$

The interesting test sets are those where α_{L} and α_{H} differ by several orders of magnitude and the required relative error is 10^{-8} or better, with no lower limit.

This set of points and weights will be a function of four input parameters: the power m; α_{L}; α_{H}; and the required precision.

The requirements will be met by choosing three variable parameters: essentially the smallest and largest r_k and the number of points.

3.2 The discretization error

For test functions with α well in the interior of the required range, a well-designed quadrature will have an oscillating error, with the highest possible number of nodes. In this range, the error is fairly insensitive to the end points $\alpha_{\mathrm{L}}, \alpha_{\mathrm{H}}$, and it is simpler to design the discretization error for the test set $T(m, -\infty, \infty)$. Scaling-symmetry suggests that an exponential radial grid is used. The variable substitution

$$r = \mathrm{e}^t \ , \tag{11}$$

$$\int_0^\infty f(r) \, \mathrm{d}r = \int_{-\infty}^\infty f[r(t)] \mathrm{e}^t \, \mathrm{d}t \ , \tag{12}$$

together with the infinite quadrature

$$r_k = \mathrm{e}^{kh} \ , \tag{13}$$

$$w_k = r_k \ , \tag{14}$$

$$S = \sum_{k=-\infty}^{\infty} w_k f(r_k) \ , \tag{15}$$

is easily seen to lead to an error that is periodic in $\ln \alpha$, with the period $\Delta \ln \alpha = 2h$ and an average value of 0. Thus it is, if not optimal, at least very close to an optimal solution, when boundary effects are ignored.

The size of the discretization error is easily deduced from a quantitative analysis along the same lines as the sampling theorem, together with elementary Fourier transform theory: the relative discretization error oscillates with the amplitude

$$R_{\mathrm{D}}^{(m)} \approx \left| \frac{\Gamma[(m+3)/2 - \pi i/h]}{\Gamma[(m+3)/2]} \right| \ . \tag{16}$$

The integral could be computed exactly from the discrete sample if the Fourier transform of the integrand had support within the maximum bandwidth allowed by the sampling theorem. The formula follows from the assumption that the error is completely dominated by the lowest-frequency Fourier components outside this band width.

Gauss' duplication formula provides a good estimate of the absolute value of the gamma function with complex argument:

$$R_{\mathrm{D}}^{(0)} \approx \frac{4\sqrt{2}\pi}{h} \mathrm{e}^{-\pi^2/2h} \ , \tag{17}$$

$$R_{\mathrm{D}}^{(m)} \approx \{\Gamma(3/2)/\Gamma[(m+3)/2]\}(\pi/h)^{m/2} R_{\mathrm{D}}^{(0)} \ . \tag{18}$$

This formula is very accurate, as verified by numerical experiments.

3.3 The truncation error from the largest r_k value

The use of an upper limit $k \leq k_{\mathrm{H}}$ instead of ∞ causes a truncation error which is largest for the test function with $\alpha = \alpha_{\mathrm{L}}$. The numerical experiments show that this error is in all cases smaller than the approximate integral to the right of $r_{k_{\mathrm{H}}}$, which gives a relative error less than

$$R_{\mathrm{L}} \approx \Gamma[(m+3)/2](\alpha r_{k_{\mathrm{H}}}^2)^{\frac{m+1}{2}} \mathrm{e}^{-\alpha r_{k_{\mathrm{H}}}^2} \ . \tag{19}$$

The truncation error is usually more than an order of magnitude smaller than this, but it also varies very rapidly with the choice of $r_{k_{\mathrm{H}}}$ – thus, this formula is good enough for determining the upper cutoff. There seems to be no reason for modifying the distribution of points near this end point.

3.4 The truncation error from the smallest r_k values

At the lower end of the summation, the effect of a truncation is quite different. Here, the truncation error is largest for test functions with $\alpha = \alpha_{\mathrm{H}}$, and it is also very dependent on m. To get an efficient distribution of points in this region, the quadrature scheme is modified in two ways. First, the distribution is made much more even close to the origin, by a slightly different variable substitution

$$r = c(\mathrm{e}^t - 1) \ , \tag{20}$$

$$\int_0^\infty f(r)\,\mathrm{d}r = \int_0^\infty f[r(t)]c\mathrm{e}^t\,\mathrm{d}t \ , \tag{21}$$

and thus

$$r_k = c(\mathrm{e}^{kh} - 1) \ , \tag{22}$$

$$w_k = r_k + c \ , \tag{23}$$

$$S = \sum_{k=0}^{\infty} w_k f(r_k) \ . \tag{24}$$

This modification has a negligible effect on the previous error analysis.

Second, the first few weights are further modified by multiplying them with the weights of Gregory's semiinfinite quadrature formula. The Gregory formula is obtained from the Euler–Maclaurin one by replacing the derivatives in the end points by asymmetric difference formulae using the few points at the very end. In our case, we used the three points closest to the origin (and also the origin itself, for $l = -2$).

The resulting truncation error, R_{H}, has been determined experimentally to be well-described by the formula

$$\ln(1/R_{\mathrm{H}}) + \frac{m+3}{2} \ln \alpha_{\mathrm{H}} r_1^2 = D_{\mathrm{m}} \ , \tag{25}$$

and the values of D_{m} were found to be $D_{-2} = 9.1$, $D_0 = 1.9$, $D_2 = -1.0$ and $D_4 = -2.3$. Equation (25) is used to define the range of the radial grid; however, it can also be used to determine how higher-order angular grids can be reduced without any loss of accuracy near the nucleus. A similar reduction based on an ad hoc approach as defined by a so-called crowding factor has been used elsewhere [8] but with no control over the error caused by the truncation of the angular grid.

3.5 The recipe

Given a specific power, m, and the required relative precision, R, a step size, h, is found for which the discretization error is $R_{\mathrm{D}} = R$. Given the exponent α_L of the most diffuse test function, determine the outermost point, $r_{k_{\mathrm{H}}}$, such that $R_{\mathrm{L}} \approx R$. Given the exponent α_{H} of the most compact test function, determine the point r_1 such that $R_{\mathrm{H}} \approx R$. From these parameters, we obtain

$$c = r_1/(\mathrm{e}^h - 1) \ , \tag{26}$$

$$k_{\mathrm{H}} = \ln(1 + r_{\mathrm{H}}/c)/h \ . \tag{27}$$

If $m \neq -2$, the point $r_0 = 0$ is left out, so the number of points is k_{H} (which, of course, is rounded to the nearest integer). For $m = -2$, this point must be included.

4 Results and discussion

In order to compare the new scheme with the ones studied in Sect. 2, we specified the exponent range to $[0.1, 10^5]$, i.e. 6 orders of magnitude, and then adjusted the requested accuracy to get a number of quadrature points close to 50, 100 and 200 points. However, it turned out that even with an error as low as 10^{-14}, we needed only 128 points. Since it would be pointless to increase the precision of the formulae beyond that allowed by the machine precision, we increased the requested range and found a suitable comparison case with an error of 10^{-14} and an exponent range of 14

orders of magnitude and 197 integration points. The results are presented in Figs. 4–6.

The design parameters of the new grid include the angular dependence through l. Usually, a direct-product grid is used for the 3D integration, and the grid must be able to handle integrands with many different angular dependences. If this is the case, a "hybrid" grid must be used for the radial integration.

We compare here the results of the normalization integrals for an s, a p and a d function for which the radial grid contains 102, 90 and 85 points, respectively, for a requested range of accuracy of 0.1–10^5 and a largest relative error of 10^{-12} (Fig. 5). It is observed that the new radial grid provides us with the requested accuracy. The lower angular momentum functions require a larger grid than the higher angular momentum functions for the same exponent range and accuracy. The parameters h, r_1 and r_k of the grids were $(0.152, 5.95\times 10^{-7}, 17.31)$, $(0.140, 1.03\times 10^{-5}, 17.31)$, and $(0.131, 4.40\times 10^{-5}, 17.31)$ for the s, p and d functions, respectively. Here we observe that the lower angular momentum functions require a longer range for r, while the higher angular momentum functions require a smaller h. In order to create a hybrid grid which integrates the given basis set not worse than some given threshold, the extreme values have to be used in the construction of the final basis set.

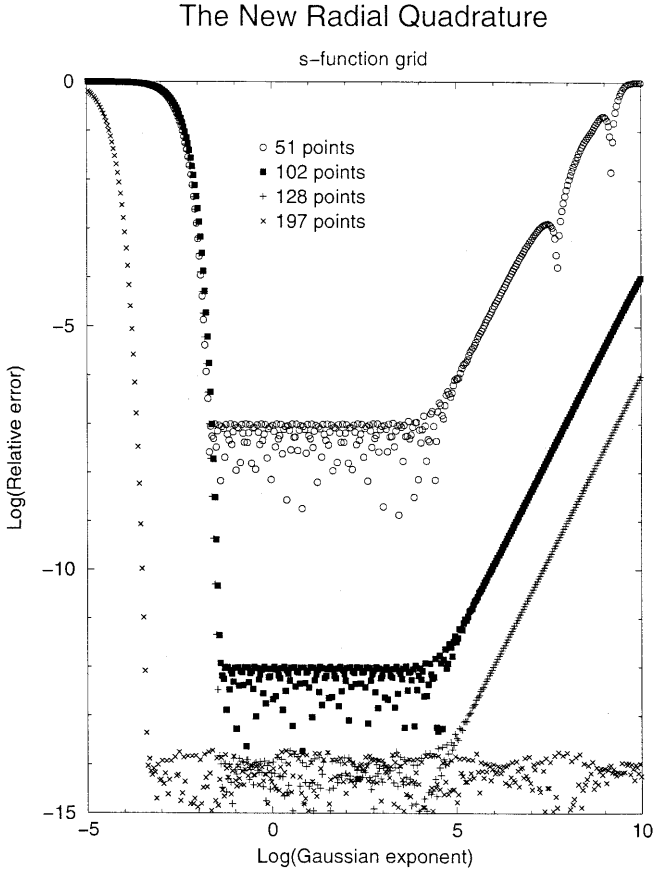

Fig. 4. The logarithm of the integrated error as a function of the logarithm of the Gaussian exponent of s functions as obtained for 51, 102, 128 and 197 radial quadrature points for the new radial quadrature

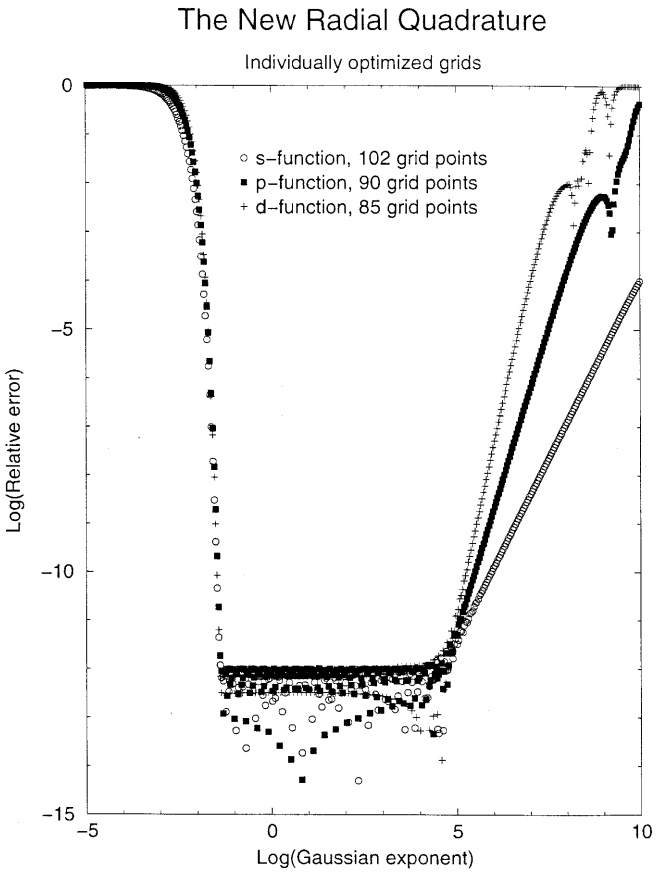

Fig. 5. The logarithm of the integrated error as a function of the logarithm of the Gaussian exponent of s, p and d functions as obtained for the new radial quadrature optimized for each individual angular shell

The result of such a hybrid quadrature is presented in Fig. 6. In this scheme we have taken the h value of the d functions and the r_1 value of the s function. The resulting grid has 118 points.

The error is no longer uniformly limited to 10^{-12} over all the values of l, so this grid cannot be optimal for the extended test set with several l values. In fact, that is probably impossible to achieve with a direct-product grid. However, no error in the requested Gaussian exponent range is larger than the requested largest acceptable error. As expected, the s functions are integrated to an accuracy better than requested in the desired Gaussian exponent range and the higher order angular functions will have an accuracy which extends far beyond the requested Gaussian exponent range.

The size of the complete grid can be cut down by using the individual $r_1(l)$ values to determine the size of the angular grid. As can be seen in Fig. 7, there is hardly any loss in accuracy.

5 Conclusions

The proposed quadrature offers a near-optimal solution to a well-defined class of "tactical" problems. However, it is clear that the search for very efficient numerical

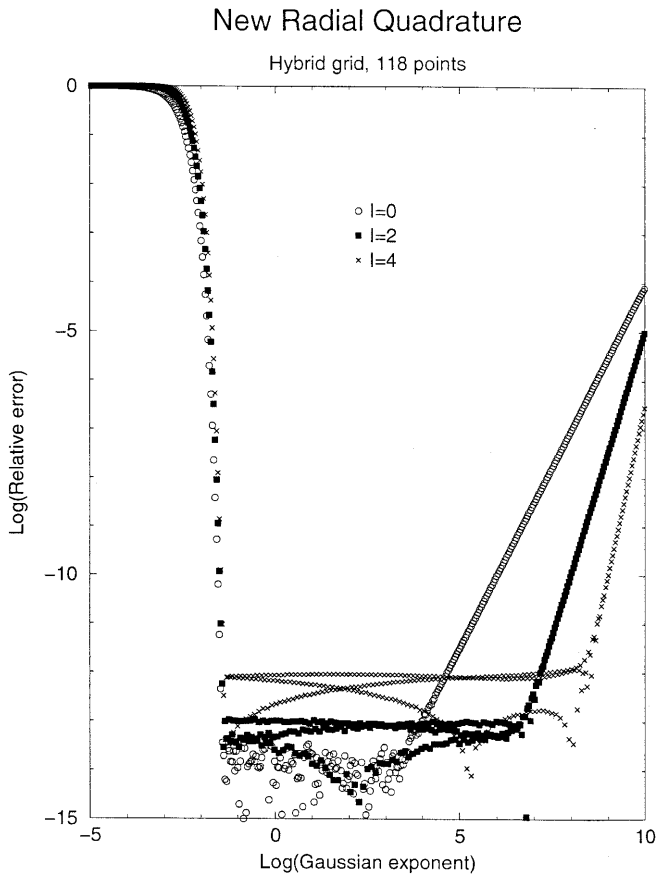

Fig. 6. The logarithm of the integrated error as a function of the logarithm of the Gaussian exponent of *s*, *p* and *d* functions as obtained in a 118 hybrid radial quadrature designed to integrate all functions no worse than the requested accuracy

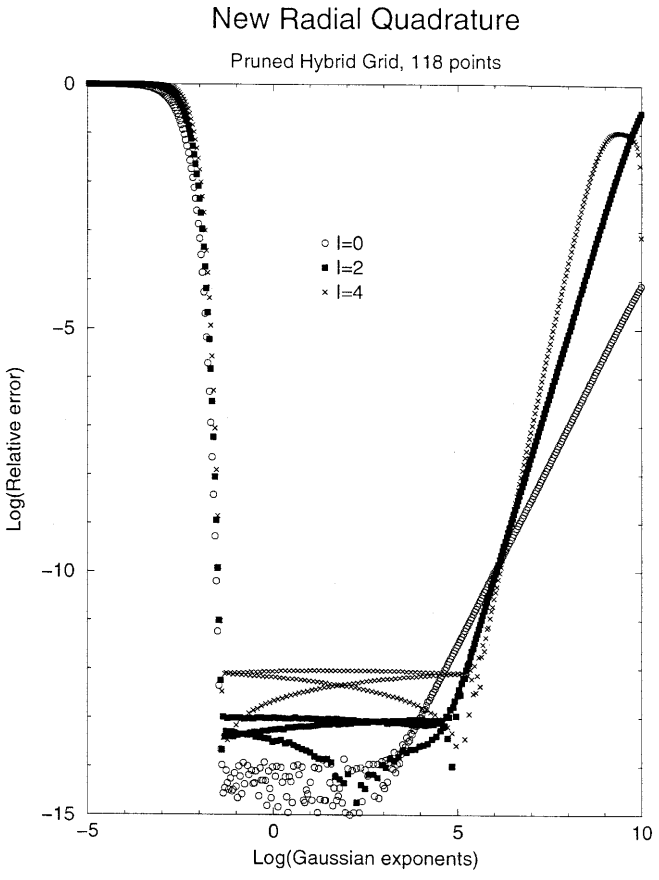

Fig. 7. The logarithm of the integrated error as a function of the logarithm of the Gaussian exponent of *s*, *p* and *d* functions as obtained in a 118 hybrid radial quadrature points approach for the new radial quadrature evoking the controlled angular pruning as suggested by the truncation formula for radial quadrature points close to the nuclei

integration techniques for quantum chemical calculations must be in the "strategical" direction. A large number of integrals, with very different size and different distribution in space, must be computed. The integrals must therefore be divided up in different classes, of which some may be ignored completely, others treated by low precision and a few must be computed with the highest accuracy. The possibility of such screening is intricately involved with the partitioning scheme. The choice of integration method within the regions depends strongly on the partitioning scheme, and it is not at all obvious that a radial-times-angular grid is the correct tactical choice for each region. An adaptive integrator using the finite element method may be the final choice.

We have initiated a study of useful known, and promising new, integration schemes; however, we addressed only the radial integration problem itself. For this problem, we argue that a flexible scheme, with specified accuracy and range of applicability as parameters, can be used. The family of radial grids presented here is parameterized by the required accuracy in a test set of integrals and by the range of exponents and the angular dependence of the integrands in this test set. Simple formulae define a grid such that the relative error of any integral in the test set is smaller than or equal to the specified threshold. The approach gives a near-optimal grid for purely radial integration of the type that is encountered, for example, in DFT calculations.

This optimality is by necessity compromised when such a grid is used as part of a direct-product grid of radial-times-angular point sets. Our approach is still useful: at least for smaller l quantum numbers, grid parameters can be selected from those which are optimal for the smallest and largest l values to result in a grid that integrates several functions within the specified accuracy. It is no longer guaranteed that the number of integration points is very close to the minimum possible, but it should not become much larger. Also, the grid parameters make it possible to use a composite grid, where fewer angular points are used close to the nucleus.

The requirement that also very high l quantum numbers should be integrated correctly results from the usual strategy of breaking up the space into smaller integration regions. If these regions are very nonspherical, and if the switching functions are sharp, this puts very large demands on the angular grid and also, to some extent, compromises the optimality of the radial grid. It is argued that the reverse relation may also be true: if the radial grid also allows high precision for more diffuse functions, smoother switching functions may be used.

Acknowledgements. This study was supported by the Swedish Natural Research Council (NFR), by the Ministero dell'Università e della Ricerca Scientifica e Tecnologica and by the European Union through contract HPRN-CT-1999-00005 within the RTN program.

References

1. Boys SF (1950) Proc Roy Soc A 200: 542
2. McMurchie LE, Davidson ER (1978) J Comput Phys 26: 218
3. Obara S, Saika A (1986) J Chem Phys 84: 3963
4. King HF, Dupuis M (1976) J Comput Phys 21: 144
5. Dupuis M, Rys J, King HF (1976) J Chem Phys 65: 111
6. Rys J, Dupuis M, King HF (1983) J Comput Chem 4: 154
7. Becke AD (1988) J Chem Phys 88: 2547
8. Murray CW, Handy NC, Laming GJ (1993) Mol Phys 78: 997
9. Treutler O, Ahlrichs R (1995) J Chem Phys 102: 346
10. Mura MM, Knowles PJ (1996) J Chem Phys 104: 9848
11. Delley B (1996) J Comput Chem 17: 1152
12. Ishikawa H, Yamamoto K, Fujima K, Iwasawa M (1999) Int J Quantum Chem 72: 509
13. Stratmann RE, Scuseria GE, Frisch MJ (1996) Chem Phys Lett 257: 213
14. Yamamto K, Fujima K, Iwasawa M (1997) J Chem Phys 108: 8769
15. Krack M, Köster AM (1998) J Chem Phys 108: 3226
16. Tozer DJ, Handy NC (1998) J Chem Phys 109: 10180